dictions are nearly exact; they are limited only by the accuracy of the equation of state, and the lack of perfect agreement is due more to experimental error than anything else. The pressure and temperature sensor are accurate to about $\pm 2\%$ of the range shown; the equation of state used is capable of predicting pressure within $\pm 0.5\%$ of its range (5000 psi), given temperature and specific volume.

References

[1] Dodge, B. F., *Chemical Engineering Thermodynamics* (McGraw-Hill Book Co., Inc., New York, 1944).

[2] Douslin, D. R., Harrison, R. H., Moore, R. T., and McCullough, J. P., "Tetrafluoromethane: PVT and intermolecular potential energy relations," J. Chem. Phys. **35**, 1357–1366 (1961).

[3] Tech. Bull. #X-34, E. I. Du Pont De Nemours and Co., Inc., "Freon" Products Div. (July 29, 1960).

Correlation of Radar Attenuation with Rocket Exhaust Temperature

DANIEL E. ROSNER*
AeroChem Research Laboratories, Inc., Princeton, N. J.

Nomenclature

a_j	=	exit plane radar attenuation
A, B, D	=	terms defined by Eq. (6)
c^*	=	characteristic velocity of propellant
C_r	=	recombination rate parameter $\equiv \alpha_{r,c} n_{e,c} d_t / c^*$
d	=	local diameter nozzle
k	=	$d \ln(a_j/n_{e,j}d_j)/d \ln \nu_{e,j}$; cf.,Eq. (6d)
M	=	local Mach number
n	=	effective pressure exponent in solid propellant (+ additive) burning rate law
n	=	total number density
n_e	=	electron number density
p	=	local pressure; $\bar{p} \equiv p/p_c$
R	=	universal gas constant
T	=	local static temperature
V	=	ionization potential of the ion's parent molecule
V_a	=	apparent ionization potential; $V_a \equiv -2R\, d(\ln a_j)/d(1/T_j)$
X_e	=	electron mole fraction n_e/n; $\bar{X}_e \equiv X_e/X_{e,c}$
α_r	=	recombination coefficient
γ	=	specific heat ratio (assumed constant)
θ_N	=	half-angle of conical expansion section
ν_e	=	electron-neutral collision frequency
ω	=	(circular) frequency of electromagnetic radiation
ω_p	=	plasma frequency

Subscripts

a	=	apparent
C_r	=	at constant C_r
c	=	in chamber
e	=	pertaining to electrons
eq	=	in local thermochemical equilibrium
j	=	at nozzle exit plane
V/RT_c	=	at constant V/RT_c
∞	=	ambient

Introduction

THE use of high-energy propellants and propellant additives can increase tracking and communication difficulties experienced when electromagnetic waves pass through a rocket exhaust plume. Attempts to understand the causes are inevitably complicated by the need to account for many simultaneous physicochemical and gasdynamic effects.[1–5] However, as a step in this direction, we consider those limiting cases amenable to theoretical analysis. In the present case, we shall assume that the dominant effect of a change in propellant formulation is to alter the combustion chamber temperature T_c and, hence, the extent of thermal ionization of an alkali-metal impurity already present in the propellant. Even here, a number of distinct phenomena must be included simultaneously, viz., the effects of altered T_c and p_c on 1) the equilibrium electron number density $n_{e,c}$ in the chamber, 2) the point within the nozzle at which the electron concentration "freezes," and 3) the collision frequency $\nu_{e,j}$ of electrons at the exit plane. Our limited object is to predict the local slope of a plot of the logarithm of exit-plane radar attenuation vs the reciprocal of the exhaust gas temperature for a fixed-geometry motor, and to define the conditions under which the resulting "apparent ionization potential" V_a bears a simple relationship to the actual ionization potential V of the alkali impurity atom.

Analysis

In traversing each unit length of rocket exhaust, an electromagnetic signal of prescribed frequency ω is attenuated by an amount depending on two plasma properties of this gas[7,8]: the plasma frequency ω_p ($\propto n_e^{1/2}$) and the electron-neutral collision frequency ν_e. Consequently, to predict V_a it is necessary to examine the nature of the attenuation law $a_j(\omega, \omega_p, \nu_e)$ and the way in which the exit-plane electron number density $n_{e,j}$ and total collision frequency $\nu_{e,j}$ respond to changes in T_c (and, hence, T_j). For this purpose, it will suffice to focus attention on functional form as opposed to absolute values. (Use will be made of the author's nonequilibrium nozzle flow theory,[3,4] to which the reader is directed for a more detailed exposition of the underlying assumptions.) Pressure dependencies are retained since, for solid propellant systems, a change in T_c will change p_c by an amount related to the effective pressure index n.[9] By equating the mass rate of hot gas generation ($\propto p_c^n$) to the mass flow rate through a supercritical nozzle ($\propto p_c T_c^{-1/2}$), one obtains the power law $p_c \propto T_c^{1/2(1-n)}$, which is incorporated in the following analysis and is taken to define n (which may be changed by an additive). By formally setting $n = -\infty$, wherever it appears, the results of the present analysis may be applied to (liquid-propellant) systems in which a change in p_c need not accompany a change in T_c. The effects of small changes in γ and mean molecular weight are neglected throughout.

The exit plane attenuation a_j is taken to be proportional to the electron "optical" depth, $n_{e,j}d_j$, in accord with the approximate law[4,7]

$$a_j \propto (n_{e,j}d_j) \cdot [\nu_{e,j}/(\omega^2 + \nu_{e,j}^2)] \qquad (1)$$

Although $\nu_{e,j}$ is linearly proportional to p_j, its temperature dependence (at constant composition) is determined by that of the electron-neutral cross section for the dominant electron scatterer in the gas. This species is $H_2O(g)$ in the cases discussed below, so that[7] $\nu_e \propto pT^{-3/2}$. It is convenient to consider $n_{e,j}$ as the product of the total number density ($n_j \propto p_j T_j^{-1}$), the equilibrium electron mole fraction in the chamber, and $\bar{X}_{e,j} \equiv X_{e,j}/X_{e,c}$, which accounts for the electron-ion recombination lag during the nozzle expansion, i.e.,

$$n_{e,j} = n_j \cdot X_{e,c} \cdot \bar{X}_{e,j} \qquad (2)$$

Subject to the assumptions of 1) weak ionization of the impurity, and 2) negligible negative ion concentrations, the Saha equation provides the functional dependence

$$X_{e,\mathrm{eq}} \propto p^{-1/2} T^{5/4} \exp(-\tfrac{1}{2} V/RT) \qquad (3)$$

Local ionization equilibrium is approximately maintained in the nozzle until a region is reached beyond which the electron

Received September 10, 1964, revision received March 3, 1965, This research was supported in part by the U. S. Air Force. Rome Air Development Center under Contract No. AF 30(602)-3142. This paper is a revised version of AeroChem TP-89 (May 1964). The author is indebted to H. Silla for his helpful discussions of existing radar attenuation measurements.

* Aeronautical Research Scientist. Associate Fellow Member AIAA.

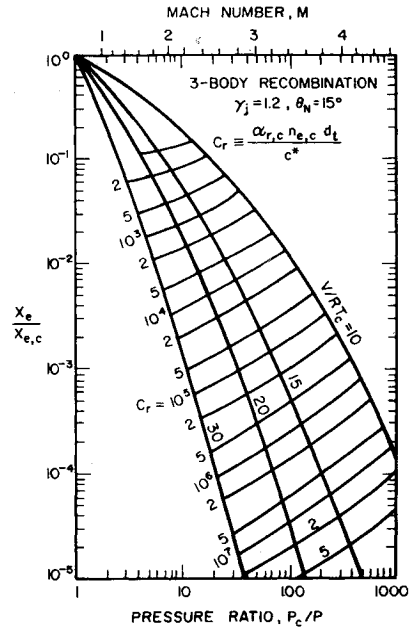

Fig. 1 Freeze-point locations[3, 4] on the $\bar{X}_e$-$\bar{p}^{-1}$ plane.

mole fraction remains nearly constant.[3, 4, 6] Since this "freeze" is particularly abrupt for the 3-body recombination (the mechanism considered here), $\bar{X}_{e,j}$ may be equated to the value of $\bar{X}_e$ at the freeze point. Freeze-point locations[3] are compactly represented in Fig. 1 ($\gamma_j = 1.2$, $\theta_N = 15°$). It is seen that $\bar{X}_{e,j} = \bar{X}_{e,j}(V/RT_c, C_r)$, where the dimensionless recombination rate parameter C_r may be interpreted as the ratio of the characteristic flow time d_t/c^* to the electron recombination half-life $(\alpha_{r,c} n_{e,c})^{-1}$ in the chamber. Thus, when T_c is increased, two competing effects must be considered in determining the change in $\bar{X}_{e,j}$: 1) the effect of moving along a new V/RT_c equilibrium contour, and 2) the altered value of C_r which locates the freeze point on this new V/RT_c contour. According to the chain rule, this may be expressed

$$d\ln\bar{X}_{e,j} = \left(\frac{\partial \ln\bar{X}_{e,j}}{\partial \ln V/RT_c}\right)_{C_r} d\ln\left(\frac{V}{RT_c}\right) + \left(\frac{\partial \ln\bar{X}_{e,j}}{\partial \ln C_r}\right)_{V/RT_c} d\ln C_r \quad (4)$$

where the two logarithmic partial derivatives are geometric properties of the freeze-point diagram, obtained at each point

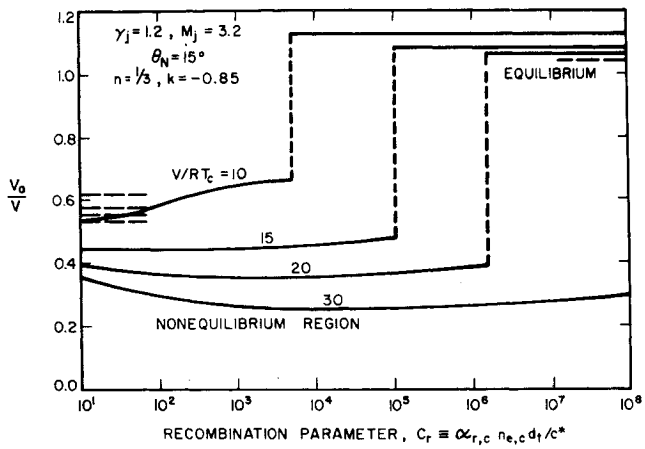

Fig. 2 Sensitivity of exit-plane attenuation to exhaust temperature in the nonequilibrium and equilibrium regimes (dashed horizontal lines at left are the frozen flow asymptotes).

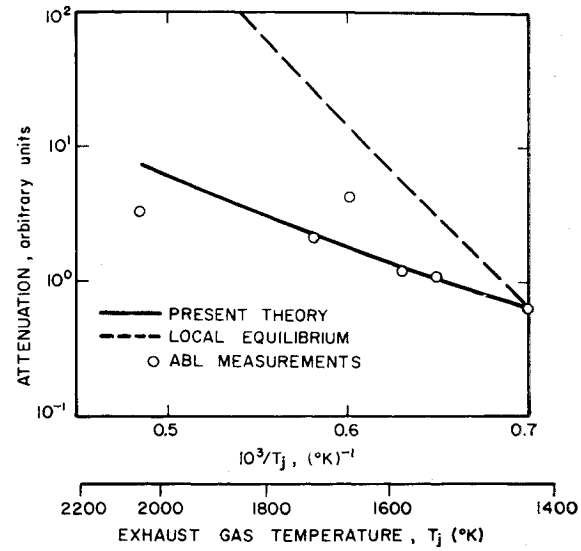

Fig. 3 Comparison of predicted and measured[10,11] dependence of attenuation on exhaust gas temperature.

by cross-plotting. The 3-body electron-ion recombination coefficient $\alpha_{r,c}$ appearing in C_r is taken to be[5] $\propto p_c T_c^{-7/2}$, and $c^* \propto T_c^{1/2}$.

Upon combining these relationships, logarithmic differentiation provides the following explicit result for the dimensionless apparent ionization potential V_a/V in the nonequilibrium regime:

$$\frac{V_a}{V} = \frac{T_j}{T_c}\left[A + B\left(\frac{\partial \ln\bar{X}_{e,j}}{\partial \ln C_r}\right)_{V/RT_c} + D\left(\frac{\partial \ln\bar{X}_{e,j}}{\partial \ln V/RT_c}\right)_{C_r}\right] \quad (5)$$

where

$$A \equiv 1 + \left[\frac{5}{2} + \frac{1 + k - \frac{1}{2}}{1 - n} - 2\left(\frac{3}{2}k + 1\right)\right]\left(\frac{V}{RT_c}\right)^{-1} \quad (6a)$$

$$B \equiv 1 - \{\tfrac{15}{2} - 3/[2(1 - n)]\}(V/RT_c)^{-1} \quad (6b)$$

$$D \equiv -2(V/RT_c)^{-1} \quad (6c)$$

$$k \equiv -1 + 2\,(\omega/\nu_{e,j})^2[(\omega/\nu_{e,j})^2 + 1]^{-1} \quad (6d)$$

(Using a similar approach, explicit expressions for the sensitivity of attenuation to impurity level, pressure level, and other quantities of interest may be obtained.[4]) In the chemically frozen flow limit ($\bar{X}_{e,j} \to 1$), the two logarithmic partial derivatives vanish, leaving only the first term in Eq. (5). The equilibrium extreme is readily treated separately and leads to the result

$$\frac{V_{a,\,eq}}{V} = 1 + \frac{T_j}{T_c}\left[\frac{5}{2} + \frac{1 + k - \frac{1}{2}}{1 - n} - 2\left(\frac{3}{2}k + 1\right)\right]\left(\frac{V}{RT_c}\right)^{-1} \quad (7)$$

The behavior of V_a/V over the entire regime from frozen flow to equilibrium flow regime can now be constructed with the help of Eqs. (5–7) and Fig. 1. A typical result is shown in Fig. 2, for the following set of parameters: $n = \frac{1}{3}$, $k = -0.85$, $M_j = 3.2$, $\gamma_j = 1.2$.

Discussion

In general, the sensitivity of exit-plane attenuation to T_j depends upon the magnitude of the recombination rate parameter C_r, and, hence, on such factors as impurity level, pressure and temperature levels, and throat diameter. Over much of the nonequilibrium regime, the slope V_a is found to be considerably smaller than V and relatively insensitive to C_r. However, beyond a critical value of C_r (which depends upon V/RT_c), V_a abruptly jumps to an equilibrium value of

the order of V, i.e., equilibrium ionization is achieved at the exit plane for all $C_r > C_{r,\text{crit}}$. (The discontinuities in Fig. 2 are, of course, a consequence of the sudden freeze approximation. Actually, each transition will be continuous[3] but quite abrupt.) The ordering and separation between the V/RT_e contours in the nonequilibrium region of Fig. 2 have two important implications. First, they indicate that a correlation of log a_j vs T_j^{-1} will exhibit greater curvature (concave upward) in the nonequilibrium regime than in either the frozen flow or equilibrium extremes. However, depending upon k, n, and the ranges of V/RT_e and C_r considered, we have found crossover points where two V/RT_e values correspond to the same V_a/V, indicating that excellent straight-line plots of log a_j vs T_j^{-1} can be obtained even in the nonequilibrium regime. Second, values of V_a in the nonequilibrium regime will be relatively insensitive to a change in V, i.e., an increase in V (hence, V/RT_e) will reduce V_a/V, leaving V_a much less changed than in either the frozen or equilibrium extremes. One, therefore, expects that the predicted dependence of a_j on T_j in the nonequilibrium regime will be relatively insensitive to the ionization potential of the principal impurity present. As a corollary, for inferring the principal ionizing species, slopes in this regime will be much less useful than slopes in the equilibrium regime.

Comparison with Attenuation Data

The parameters selected in constructing Fig. 2 define a set of conditions approximately met in recent radar attenuation experiments on aluminized, double-base, solid propellant motors,[10, 11] which covered a 650°K range in T_j and nearly a decade range in attenuation. (In keeping with the assumptions underlying Fig. 2, data for chlorine-containing propellants or for nozzle area ratios very different from 8.9 will not be considered here). In Fig. 3 the observed temperature sensitivity of the attenuation is compared, with encouraging results, to that predicted by the present idealized theory. This is done by passing the curve predicted by Eq. (5) through the lowest-temperature data point. For comparison, the much steeper curve (dashed) corresponding to local ionization equilibrium is also shown. In both cases, the impurity is assumed to be sodium ($V = 5.1$ ev), but, in accord with the previous discussion, if the impurity were potassium ($V = 4.3$ ev), slopes computed in the nonequilibrium regime would equally well represent the data. It is not necessary to accurately specify impurity level in this comparison, because the predicted slopes in the nonequilibrium regime are nearly the same over more than a four-decade range of C_r, which, subject to the foregoing assumptions, would correspond to an eight-decade range of impurity level. Of course, the impurity level determines the absolute value of the attenuation.

In correlating data, one must usually account for the fact that attenuation measurements during static firings are made somewhat downstream of the exit plane (to avoid reflections from the nozzle), so that additional expansion (if $p_\infty < p_j$) or compression (if $p_\infty > p_j$) occurs[4] before the observation point is reached. Such corrections can be made on the basis of the flow field determined by the method of characteristics.[12] Peripheral afterburning of fuel-rich exhausts and two-dimensional effects within the nozzle (invalidating simple one-dimensional flow nonequilibrium predictions) can also affect comparisons.[4]

References

[1] Spokes, G. N., "The role of aluminum and its oxides as sources or moderators of electrons in solid propellant rocket exhausts," Stanford Research Institute Rept. TDR 63 326, DDC AD 447 283 (August 1964).

[2] Kurzius, S. C. and Skinner, R. C., "Effects of solid particles on electron concentrations in a plasma," AeroChem TP-72b (March 1964); unclassified section of "Flame plasma effects study," (U), RADC–TDR- 64–263 (October 1964); secret.

[3] Rosner, D. E., "Estimation of electrical conductivity at rocket nozzle exit sections," ARS J. **32**, 1602–1605 (1962).

[4] Rosner, D. E., "Ionization in rocket exhaust plumes," AeroChem TP-85; DDC–AD 447 304 (March 1964); also *Plasma Technology, Aerospace Applications*, edited by J. Grey (Prentice Hall, Inc., Englewood Cliffs, N. J., to be published).

[5] Calcote, H. F., "Relaxation processes in plasma," *Dynamics of Conducting Gases* (Northwestern University Press, Evanston, Ill., 1960), pp. 36–50.

[6] Eschenroeder, A. Q., "Ionization nonequilibrium in expanding flows," ARS J. **32**, 196–203 (1962).

[7] Molmud, P., "Vernier exhaust perturbations on radar and altimeter systems during a lunar landing," AIAA J. **1**, 2816–2819 (1963).

[8] Balwanz, W. W., "Interaction between electromagnetic waves and flames, Part VI: Theoretical plots of absorption, phase shift, and reflection," U. S. Naval Research Lab. NRL Rept. 5388 (September 1959).

[9] Sutton, G. P., *Rocket Propulsion Elements* (John Wiley and Sons, Inc., New York, 1956), 2nd ed.

[10] Vreeland, R. W., unpublished experiments, Allegany Ballistics Lab., Cumberland, Md. (April 5, 1963).

[11] Vreeland, R. W., private communication with H. F. Calcote (November 19, 1963).

[12] Moe, M. M. and Troesch, B. A., "Jet flow with shocks," ARS J. **30**, 487–489 (1960).

Long-Time Room Temperature Tensile Creep Tests of 2014-T6 Aluminum Alloy Used In Titan II

M. J. Brown*

Martin Company, Baltimore, Md.

THE Titan II vehicle is designed to be stored at room temperature with pressurized propellant tanks for from one to three years. This design condition raises the question as to whether significant amounts of creep will occur in bare (unclad) 2014-T6 alloy, with and without welds, when subjected to a stress equivalent to 50% of the ultimate stress, for long periods of time at room temperature. Extrapolation of short-time creep data indicated that the problem was not critical, but confirmation by test was desired.

Material selected for this investigation was obtained from Martin stock in the form of 0.100-in.-thick 2014-T6 bare sheet. All of the specimens were oriented in a direction normal to the rolling direction of the original sheet. The welded specimens were prepared by Titan II manufacturing procedures, using the manual tungsten electrode, A-C inert gas-shielded Tungsten Inert Gas (TIG) method, with 4043 aluminum alloy filler wire. A welding fixture made of a copper backup bar and steel clamping plates was used to ensure properly aligned specimens. The specimens were tested in the as-welded condition (not heat-treated after welding).

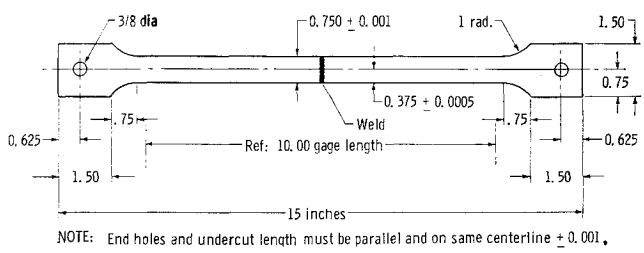

Fig. 1 Test specimen configuration.

Received September 29, 1965; revision received December 14, 1964.

* Supervisor, Materials Engineering, Engineering Laboratories.